

Supporting Information for

**Core-Shell Structured Mesoporous Silica Spheres: A New
Immobilized Strategy for Rhodium Catalyzed Asymmetric
Transfer hydrogenation**

Huaisheng Zhang, Ronghua Jin, Hui Yao, Shuang Tang, Jinglan Zhuang, Guohua Liu and Hexing Li**

Key Laboratory of Resource Chemistry of Ministry of Education, Shanghai Key Laboratory of Rare Earth
Functional Materials, Shanghai Normal University, Shanghai 200234, P. R. China

	Content	Page
Experimental	General, characterization, preparation and catalytic reaction	S2
Figure S1	FT-IR spectra of the MSN (1) and 2-3 .	S5
Figure S2	¹³ C CP MAS NMR spectra of 2-3	S6
Figure S3	²⁹ Si MAS NMR spectra of 2-3	S7
Figure S4	XPS spectra of Cp*RhTsDPEN and 3	S8
Figure S5	TG/DTA curves of DMSS and 3	S9
Table 1	Asymmetric transfer hydrogenation of aromatic ketones	S11
Figure S6	Asymmetric transfer hydrogenation of aromatic ketones	S12
Table S1	Reusability of 3 using acetophenone as a substrate	S18
Figure S7	Reusability of 3 using acetophenone as a substrate	S18
Table S2	Reusability of 4 using acetophenone as a substrate	S22
Figure S8	Reusability of 4 using acetophenone as a substrate	S22

Experimental

1. General remarks

All experiments, which are sensitive to moisture or air, were carried out under an Ar atmosphere using the standard Schlenk techniques. (*S,S*)-1,2-diphenylenediamine [(*S,S*)-DPEN], (*R,R*)-1,2-diaminocyclohexane [(*R,R*)-DACH], triethanolamine (TEA), cetyltrimethylammonium chloride (CTAC) and [Cp*RhCl₂]₂ were purchased from Sigma-Aldrich Company Ltd. Compound [(*S,S*)-DPEN-SO₂Ph(CH₂)₂Si(OMe)₃]₂, {(1*R*,1*R*)-DACH-[(CH₂PhSi(OMe)₃]₂} were synthesized according to the reported literature [a] *Chem Commun.* **2011**, 47, 2583.] The products of the ATH were analyzed by a GC using a Supelco β-Dex 120 chiral column (30 m×0.25 mm(i.d.), 0.25 μm film) or a HPLC with a UV-Vis detector using a Daicel OJ-H chiralcel columns (Φ 0.46 x 25 cm).

2. Characterization

Rh loading amount in the catalyst was analyzed using an inductively coupled plasma optical emission spectrometer (ICP, Varian VISTA-MPX). Fourier transform infrared (FTIR) spectra were collected on a Nicolet Magna 550 spectrometer using KBr method. X-ray powder diffraction (XRD) was carried out on a Rigaku D/Max-RB diffractometer with CuKα radiation. Scanning electron microscopy (SEM) images were obtained using a JEOL JSM-6380LV microscope operating at 20 kV. X-ray photoelectron spectroscopy (XPS) measurements were performed on a Perkin-Elmer PHI 5000C ESCA system. All the binding energies were calibrated by using the contaminant carbon (C_{1s} = 284.6 eV) as a reference. Liquid-state ¹H NMR, ¹³C NMR, and Solid-state ²⁹Si MAS NMR and ¹³C CP MAS NMR spectra were recorded on a Bruker AV-400 spectrometer. Elemental analysis was performed with a Carlo Erba 1106 Elemental Analyzer.

3. Preparation of Cp*RhTsDPEN-MSS (2): TEA (14.3 g, 95.6 mmol) and TEOS (1.557 g, 7.84 mmol, 85 mol % of the total amount of required TEOS), and 230.5 mg (0.461 mmol, 5 mol % of the total TEOS) of **1**, followed by heating for 20 minute at 90 °C without stirring (solution 1). Meanwhile, 2.41 mL (7.29 mmol) of CTAC and 21.7 g of water (solution 2) were preheated at 60 °C, added to solution 1, and stirred for 20 minute. The resulting solution was then left to stir overnight at room temperature. The resulting mixture was then centrifuged (10000r/min) for 10 minute, redispersed in EtOH, and extracted template. Extraction of the organic template from the mesoporous silica spheres was performed by heating the colloidal suspension for 45 minute at 90 °C in a solution containing 2.0 g of ammonium nitrate in 90 mL of absolute ethanol. After being separated *via* centrifugation (10000r/min) for 10 minute, the mesoporous silica spheres was then redispersed in EtOH and

refluxed for 45 minute in a solution of 10 mL of concentrated hydrochloric acid and 90 mL of absolute ethanol. After that the solution was filtrated and washed by absolute ethanol, the solid was dried at room temperature under vacuum overnight to afford catalyst **2** (1.02 g) as a white powder. IR (KBr) cm^{-1} : 3448.5 (s), 2979.7 (w), 2932.5 (w), 1637.4 (m), 1549.8 (w), 1500.2 (w), 1453.1 (w), 1384.3 (w), 1085.2 (s), 964.3 (m), 797.5 (m), 701.3 (w), 566.8 (w), 464.1 (s). Elemental analysis (%): C 10.22, H 3.79, N 0.97, S 0.14. S_{BET} : 762.6 m^2/g , V_{pore} : 0.68 cm^3/g , d_{pore} : 2.81 nm. ^{29}Si MAS NMR (300 MHz): Q^3 ($\delta = -101.6$ ppm), Q^4 ($\delta = -111.2$ ppm), T^2 ($\delta = -57.5$ ppm), T^3 ($\delta = -67.5$ ppm). ^{13}C CP MAS NMR (161.9 MHz): 134.6, 128.2 (Ar-C), 76.2 (NH-CH-Ph), 59.6 (OCH₃), 17.5 (CH₂-Ar), 3.4 (SiCH₃/CH₂) ppm. The FT-IR, ^{13}C CP MAS NMR, ^{29}Si CP MAS NMR spectra were presented in figure S1-S3

4. Preparation of Cp*RhTsDPEN-DMSS (3). To a stirred suspension of **2** (1.0 g) was added a solution of 2.41 mL (7.29 mmol) of CTAC and 21.7 g of water that were preheated at 60 °C and stirred for 12 hours at room temperature. Next 183.2 mg of TEOS (0.922 mmol, 10 mol % of the total TEOS) was added in four increments every 30 minute, and the resulting solution was then left to stir overnight at room temperature. The resulting mixture was then centrifuged (10000r/min) for 10 minute, redispersed in EtOH, and extracted template. After being separated *via* centrifugation (10000r/min) for 10 minute, the solids was suspended in 20 mL dry CH₂Cl₂ and NEt₃ (1.30 mL, 21.5 mmol) and [Cp*RhCl₂]₂ (0.050 g, 0.092 mmol) were added at room temperature. The resulting mixture was stirred at room temperature for 12h. The mixture was then filtered through filter paper and rinsed with excess CH₂Cl₂. After Soxlet extraction in CH₂Cl₂ solvent to remove homogeneous and unreacted start materials for 24 h, the solid was dried at 60 °C in vacuum for 12 h to afford **3** (1.14 g, 95.2% relative to **2**) as a light orange powder. ICP analysis shows that the Rh loading-amount was 4.12 mg (0.040 mmol) per gram catalyst. IR (KBr) cm^{-1} : 3439.6 (s), 2980.3 (w), 2928.7 (w), 1637.4 (m), 1561.7 (w), 1542.8 (w), 1509.6 (w), 1457.6 (w), 1384.3 (w), 1086.7 (s), 959.1 (m), 800.7 (m), 701.3 (w), 573.1 (w), 461.2 (s). Elemental analysis (%): C 12.35, H 4.03, N 0.86, S 0.13. S_{BET} : 761.0 m^2/g , V_{pore} : 0.58 cm^3/g , d_{pore} : 2.58 nm. ^{29}Si MAS NMR (300 MHz): Q^3 ($\delta = -101.9$ ppm), Q^4 ($\delta = -111.2$ ppm), T^3 ($\delta = -67.1$ ppm). ^{13}C CP MAS NMR (161.9 MHz): 134.1, 129.8 (Ar-C), 95.5 (Cp*-C), 75.1 (NH-CH-Ph), 59.6 (OCH₃), 17.5 (CH₂-Ar), 8.2 (CpCH₃), 3.4 (SiCH₃/CH₂) ppm. The FT-IR, ^{13}C CP MAS NMR, ^{29}Si CP MAS NMR, XPS and TG/DTA curves were presented in figure S1-S5

4. Preparation of Cp*RhTsDACH-DMSS (4). Prepared according to the above general procedure 3 using TsDACH-derived silane instead of TsDPEN-derived silane, the solid was dried under reduced pressure overnight to afford Cp*RhTsDPEN-IBOIHS (**4**) as a light red

powder. ICP analysis shows that the Rh loading-amount was 4.63 mg (0.045 mmol) per gram catalyst. IR (KBr) cm^{-1} : 3446.1 (s), 2941.9 (w), 2872.8 (w), 1630.4 (m), 1450.5 (w), 1410.8 (w), 1383.6 (w), 1327.9 (w), 1308.7 (w), 1089.3 (s), 961.5 (m), 803.6 (m), 576.7 (w), 462.4 (s). Elemental analysis (%): C 17.27, H 4.25, N 1.11, S 0.14. S_{BET} : 723.2 m^2/g , V_{pore} : 0.53 cm^3/g , d_{pore} : 2.59 nm. ^{29}Si MAS NMR (300 MHz): T^3 ($\delta = -67.6$ ppm), Q^2 ($\delta = -92.5$ ppm), Q^3 ($\delta = -102.1$ ppm), Q^4 ($\delta = -111.0$ ppm). ^{13}C CP/MAS (161.9 MHz): 4.3 ($\underline{\text{C}}\text{H}_2\text{-Si}$), 7.4 ($\underline{\text{C}}\text{H}_3\text{-Cp}^*$), 15.3 ($\text{Ph}\underline{\text{C}}\text{H}_2$), 23.6, 28.3 ($\underline{\text{C}}$ of cyclohexyl group without connected to N atom), 54.8 ($\underline{\text{C}}\text{H}_3\text{-O}$), 76.3, 73.0 ($\text{PhN-}\underline{\text{C}}\text{H}_2$), 93.8 ($\underline{\text{C}}\text{-Cp}$), 126.8 ($\underline{\text{C}}\text{H}$ of Ar) ppm.

5. Asymmetric transfer hydrogenation of ketones in aqueous medium. A typical procedure was as follows: The catalyst **3** (25.00 mg, 1.0 μmol of Rh based on ICP analysis), HCO_2Na (0.13 g, 0.19 mmol), ketone (0.25 mmol) and 4.0 mL water were added in a 10 mL roundbottom flask in turn. The mixture was allowed to react at 40 °C for 8h. During that time, the reaction was monitored constantly by TLC. After completion of the reaction, the magnetic catalyst was separated via centrifuge (10000 r/min) for the recycle experiment. The aqueous solution was extracted by Et_2O (3×3.0 mL). The combined Et_2O was washed with brine twice and dehydrated with Na_2SO_4 . After the evaporation of Et_2O , the residue was purified by silica gel flash column chromatography to afford the desired product. The conversion and the ee value could be determined by chiral GC using a Supelco β -Dex 120 chiral column (30 m \times 0.25 mm(i.d.), 0.25 μm film) or a HPLC analysis with a UV-Vis detector using a Daicel OJ-H chiralcel columns (Φ 0.46 x 25 cm).

Figure S1. FT-IR spectra of MSS and the catalyst 2-3.

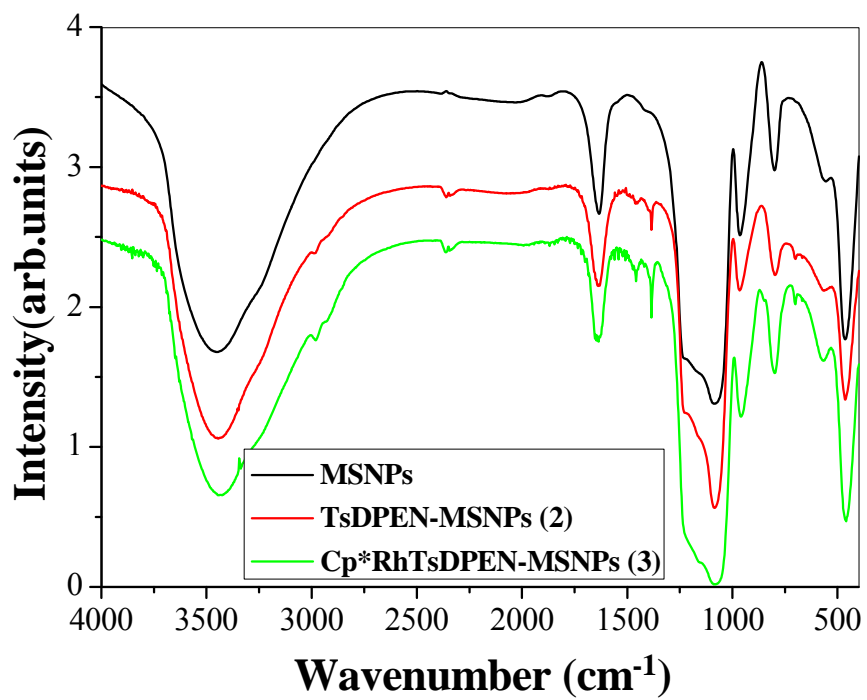


Figure S2. Solid-state ^{13}C CP MAS NMR spectra of **2-3**.

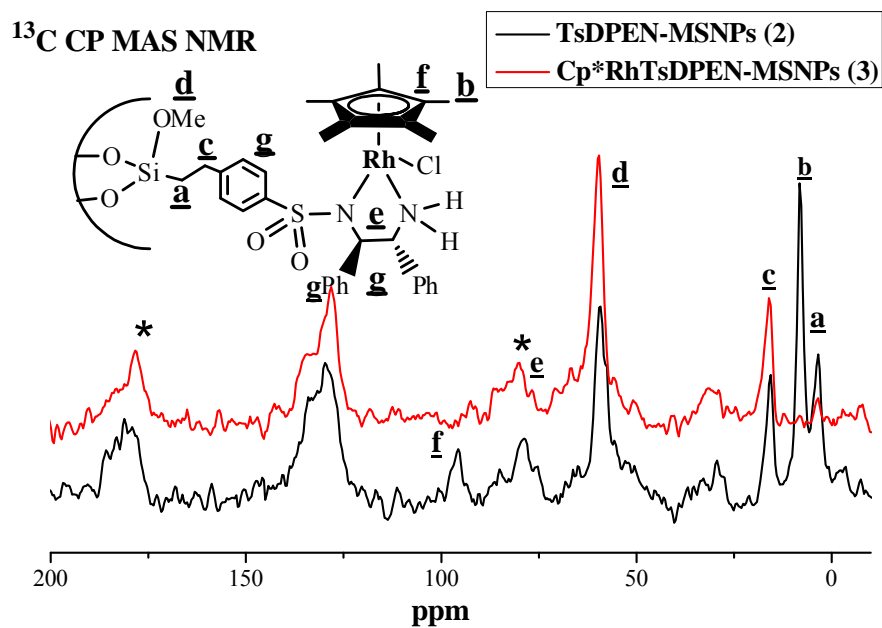


Figure S3. Solid-state ^{29}Si MAS NMR spectra of **2-3**.

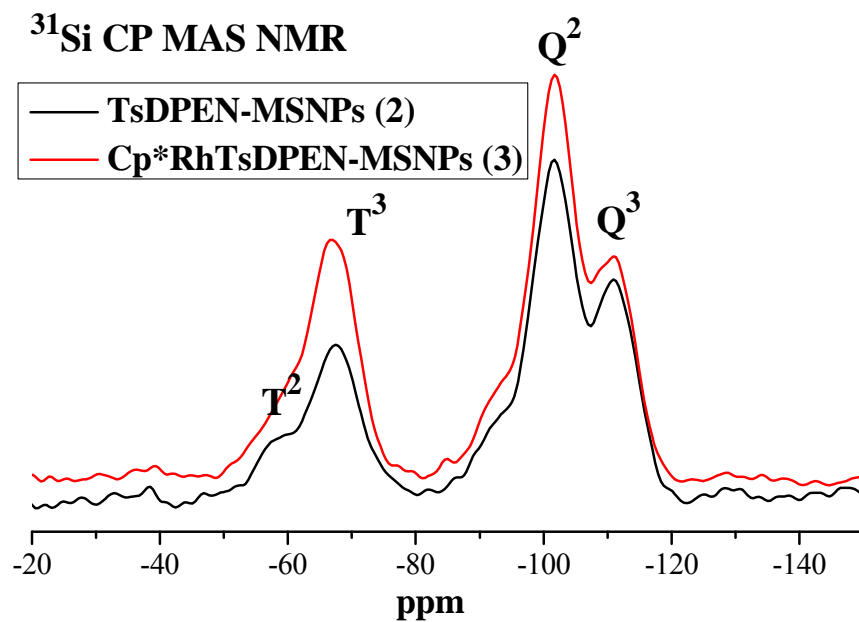


Figure 4. XPS spectra of the homogeneous Cp*RhTsDPEN and **3**.

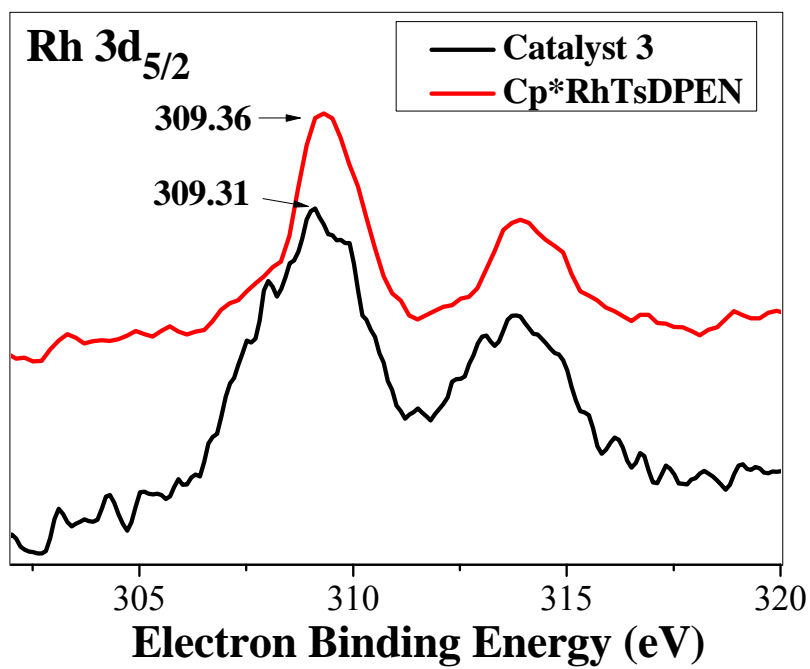
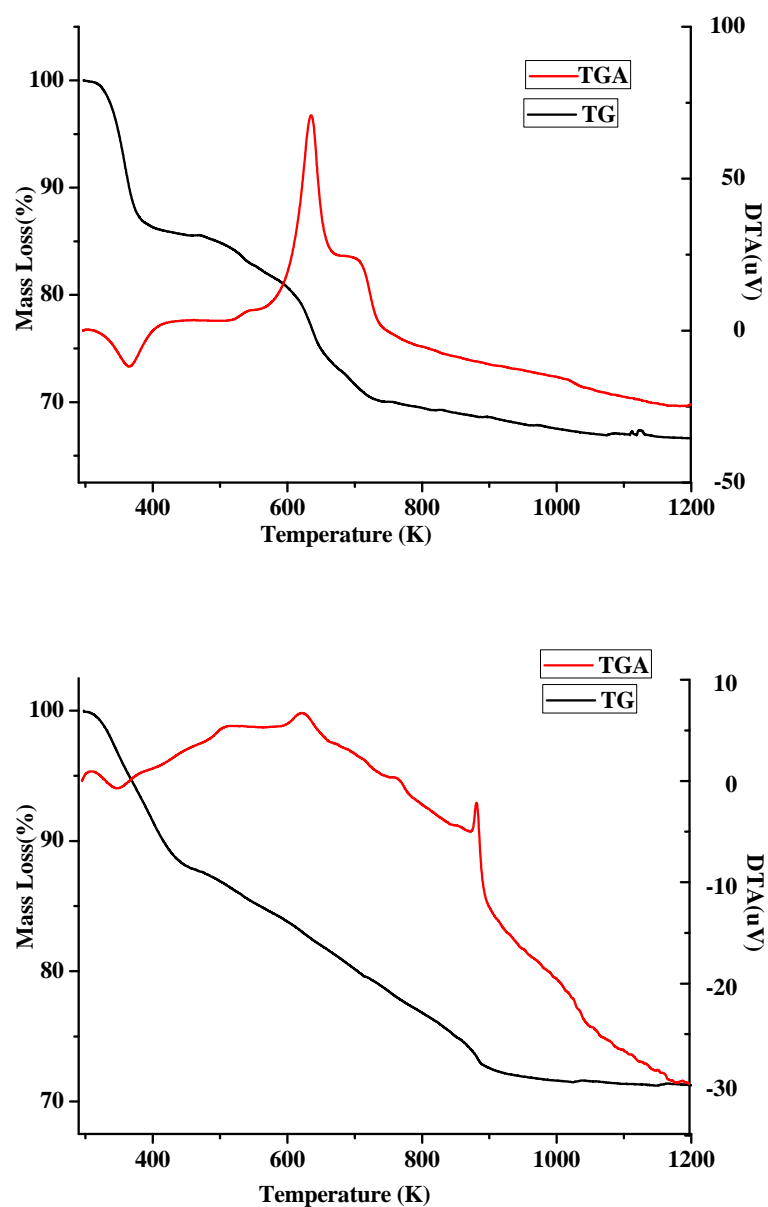


Figure S4. TG/DTA curves of the DMSS and the catalyst **3**.



Explanation: The TG/DTA curve of DMSS and the catalyst **3** were treated in the air as shown in Figure S5. An endothermic peak around 444K with weight loss of 11.9% could be attributed to the release of physical adsorption water while the another endothermic peak around 444-900K with weight loss of 16.4% could be assigned to the release of the residual CTAC surfactant (cetyltrimethylammonium chloride) in the core-shell extracted samples (V. Cauda, A. Schlossbauer, J. Kecht, A. Zürner, T. Bein, *Am. Chem. Soc.*, 2009, **131**, 11361). Apparently, totally weight loss of the residual CTAC surfactant was 16.4% in 88.1% DMSS materials when eliminated the part of water, meaning the 18.6% weight loss of the residual

CTAC surfactant per 100% materials.

In sharp contrast to TG/DTA curve of DMSS, it was found easily that a similar endothermic peak around 444K with weight loss of 14.4% in the heterogeneous catalyst **3** were strongly similar to that of parent DMSS due to the release of physical adsorption water. It was worth mentioning that two new typical exothermic peaks were combined into one complicated exothermic peak around 636-701 K with weight loss of 9.5% could be assigned to the oxidation of Cp*RhTsDPEN organic molecules (including Cp* ring and TsDPEN moiety, alkyl fragments and part of the residual CTAC surfactant). Because the totally weight loss of organic moieties (including Cp*RhTsDPEN organic molecules and the residual CTAC surfactant) was 33.0% per 85.6% DMSS materials when eliminated the part of water, meaning the whole weight loss 21.7% (including the residual CTAC plus Cp*RhTsDPEN organic molecules) per 100% materials. Apparently, in sharp contrast to the weight loss of the residual CTAC surfactant in DMSS material, the true weight loss of Cp*RhTsDPEN organic molecules was 3.1% (21.7-18.6) per 100% materials.

Table 1. Asymmetric transfer hydrogenation of aromatic ketones.^[a]



Entry	Ar	Conv. (%) ^b	Ee. (%) ^b
1	Ph	>99(88)	96 (96)
2	4-FPh	>99	95(95)
3	4-ClPh	>99	95(94)
4	4-BrPh	>99	93
5	3-BrPh	97.8	95
6	4-MePh	>99	92(93)
7	4-OMePh	>99	95(97)
8	3-OMePh	>99	96(98)
9	4-CNPh	>99	89(91)
10	4-CF ₃ Ph	>99	93
11	4-NO ₂ Ph	>99	87 (88)
12	2-naphthyl	>99	95

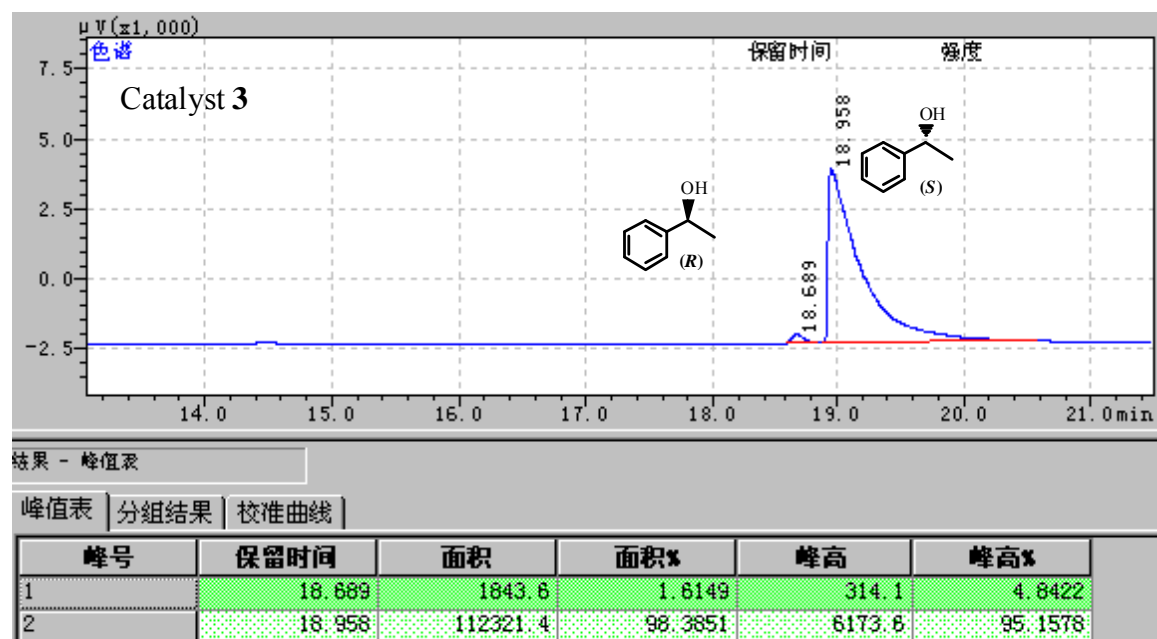
^a Reaction conditions: catalysts (25.00 mg, 1.0 μmol of Rh based on ICP analysis), HCO₂Na (0.13 g, 0.19 mmol), ketone (0.25 mmol) and 2.0 mL water, reaction temperature (40 °C), reaction time (1.0-6.0 h). ^b Determined by chiral GC or HPLC analysis (see ESI in Fig. S6).

Translation of Chinese to English is as follows:

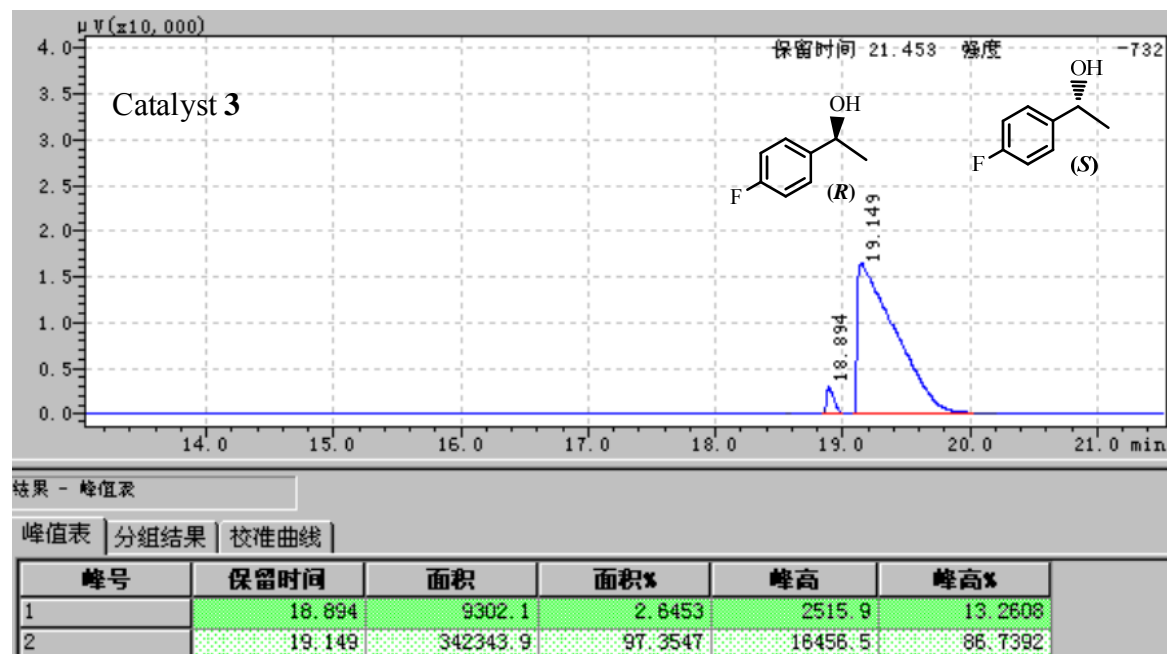
Peak	RetTime [min]	Area	Area%	Heigh	Heigh%
峰号	保留时间	面积	面积%	峰高	峰高%
1	18.474	235819.9	92.0500	13827.2	79.0885
2	19.395	9109.7	3.5589	1042.4	5.9808

Figure S6. The catalytic activity and enantiomeric excess were determined by chiral GC using a Supelco β -Dex 120 chiral column (30 m \times 0.25 mm (i.d.), 0.25 μ m film)

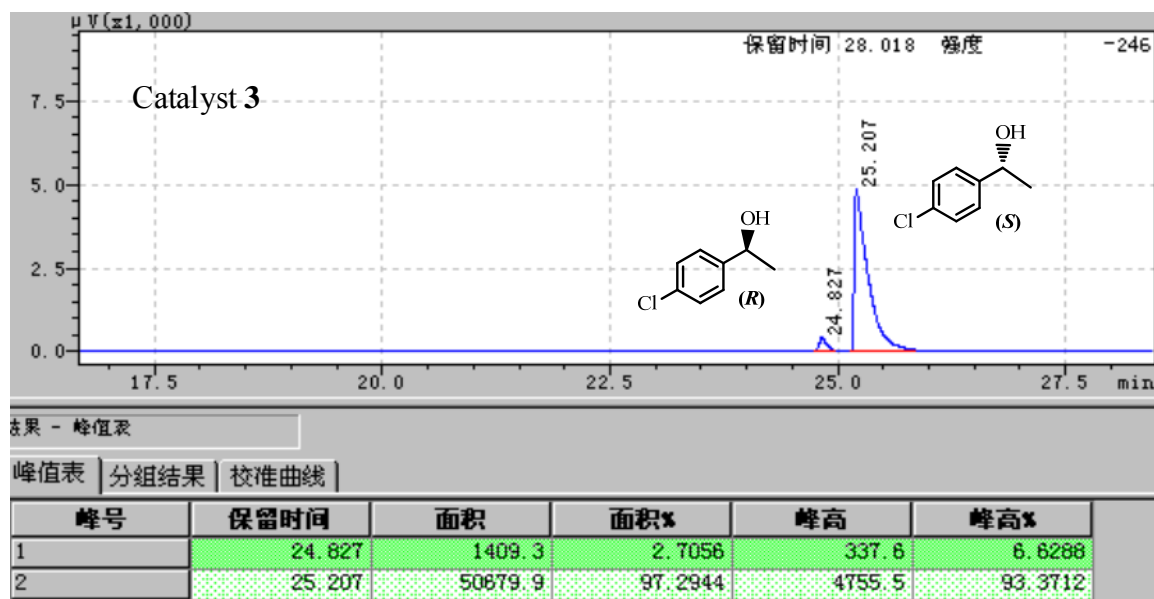
Asymmetric transfer hydrogenation of acetophenone.



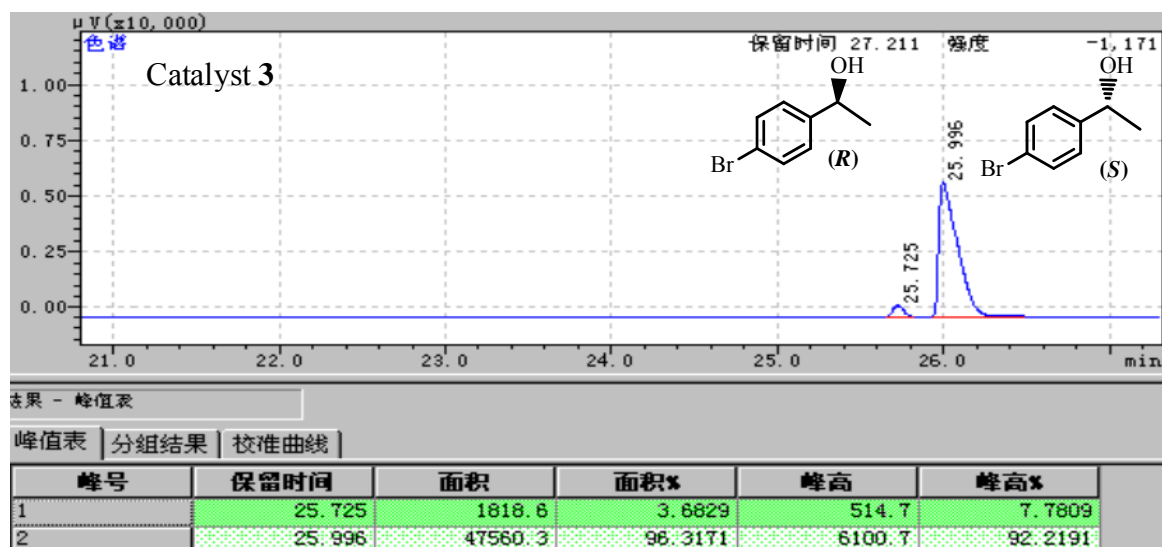
Asymmetric transfer hydrogenation of 4-fluoroacetophenone.



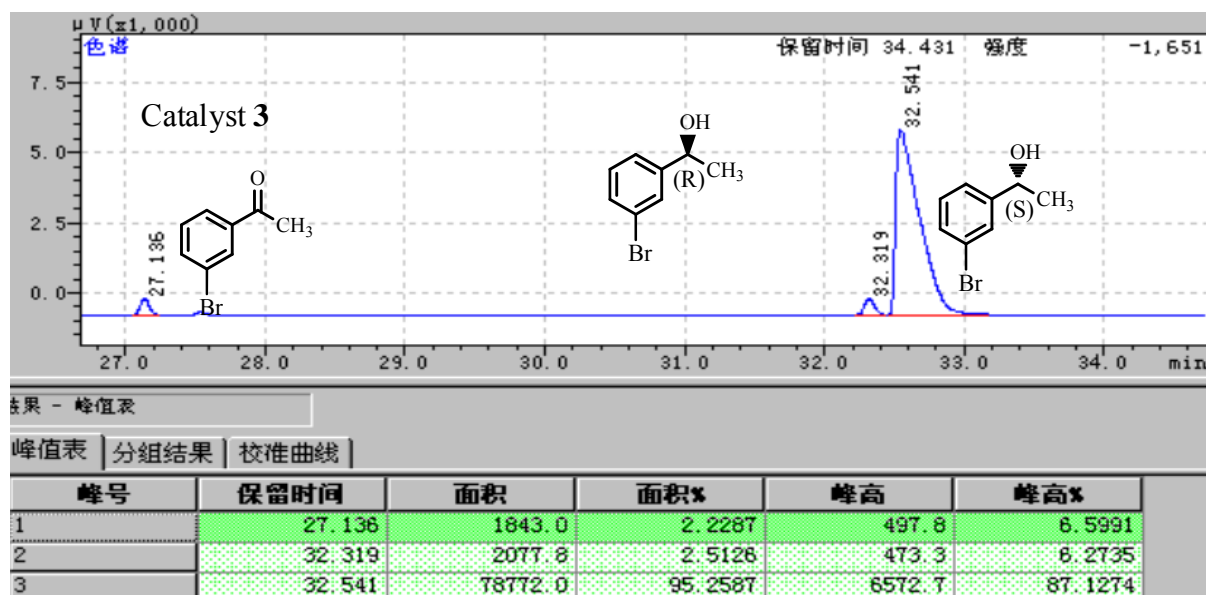
Asymmetric transfer hydrogenation of 4-chloroacetophenone.



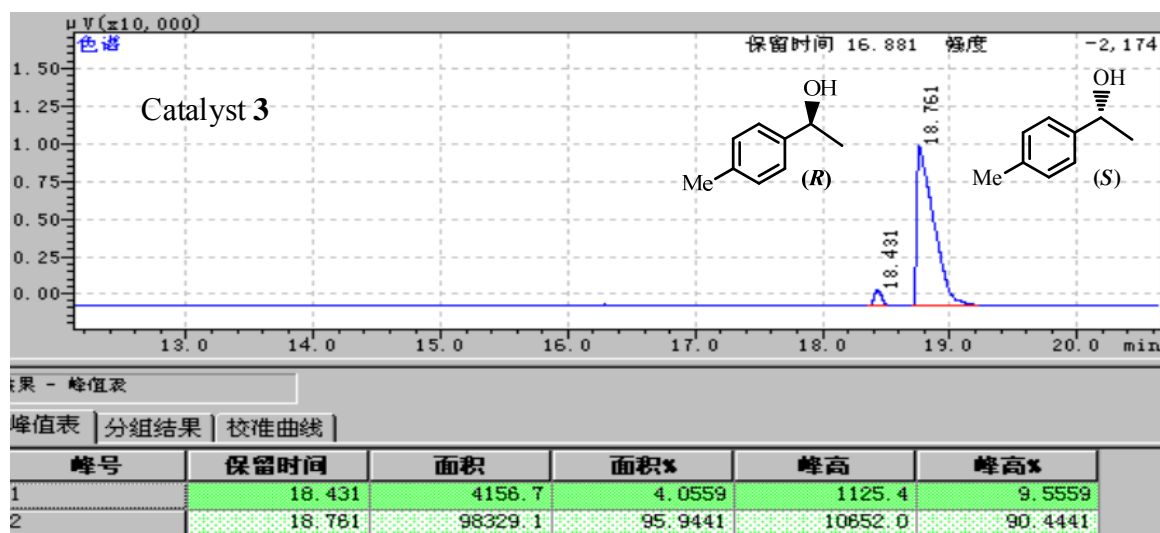
Asymmetric transfer hydrogenation of 4-bromoacetophenone.



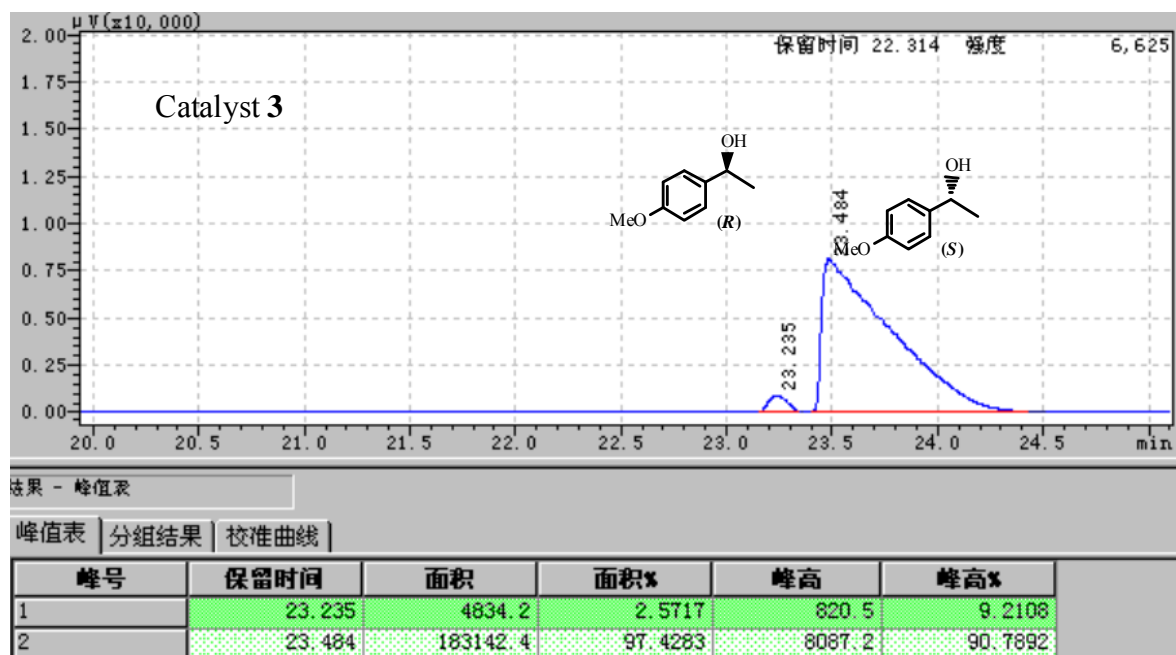
Asymmetric transfer hydrogenation of 3-bromoacetophenone.



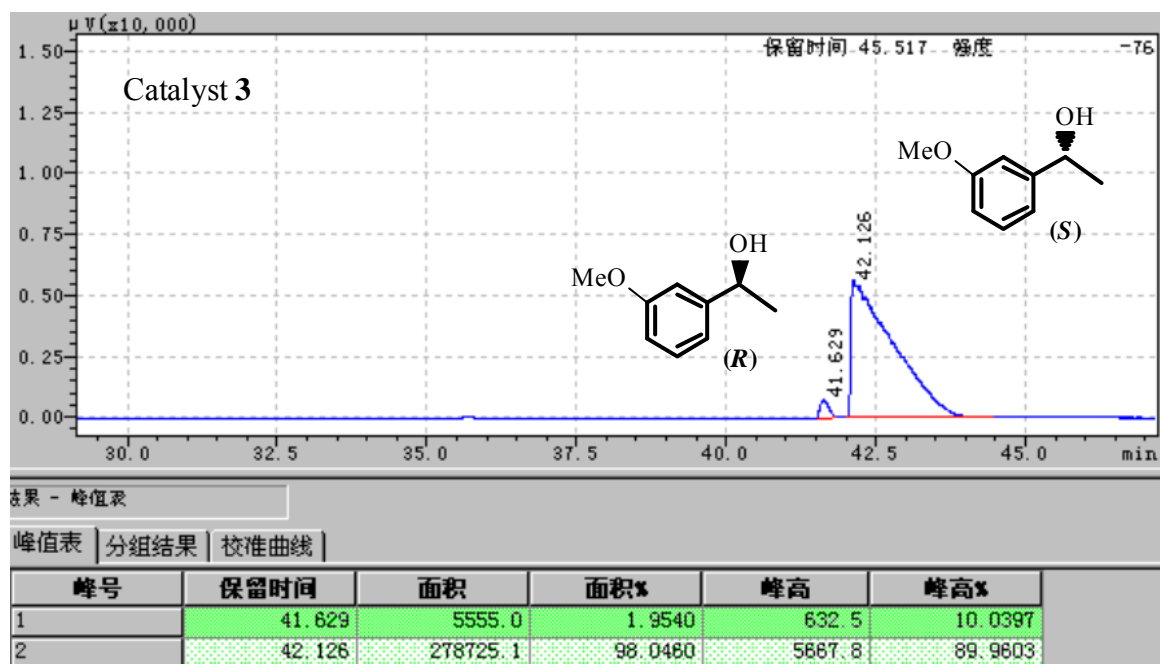
Asymmetric transfer hydrogenation of 4-methylacetophenone.



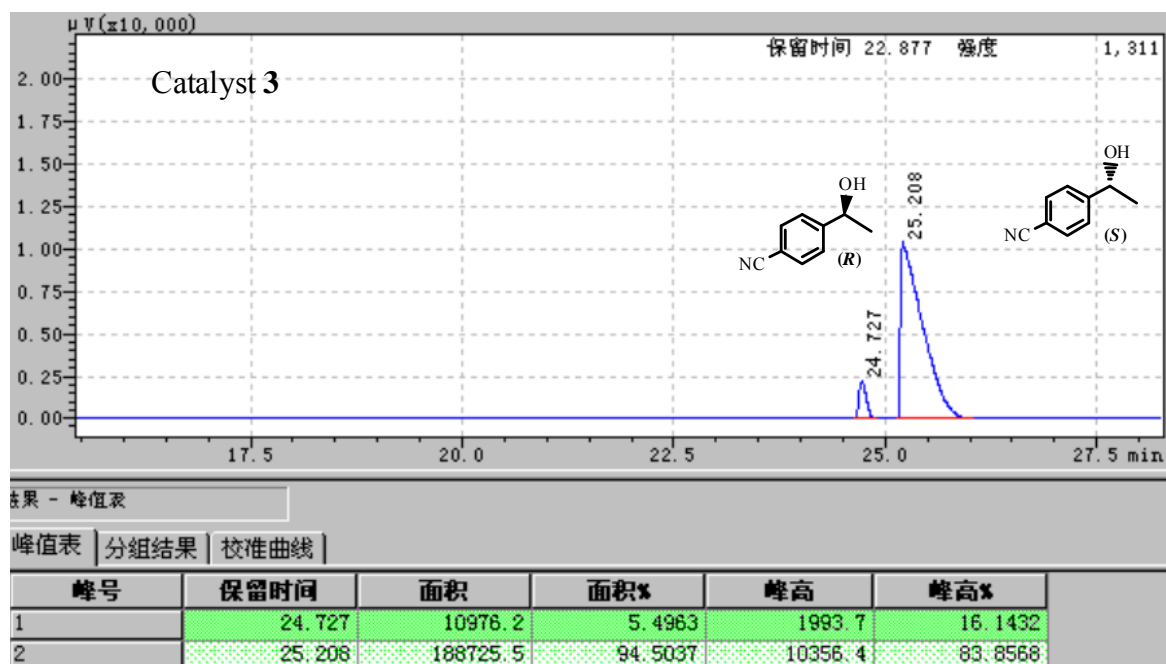
Asymmetric transfer hydrogenation of 4-methoxyacetophenone.



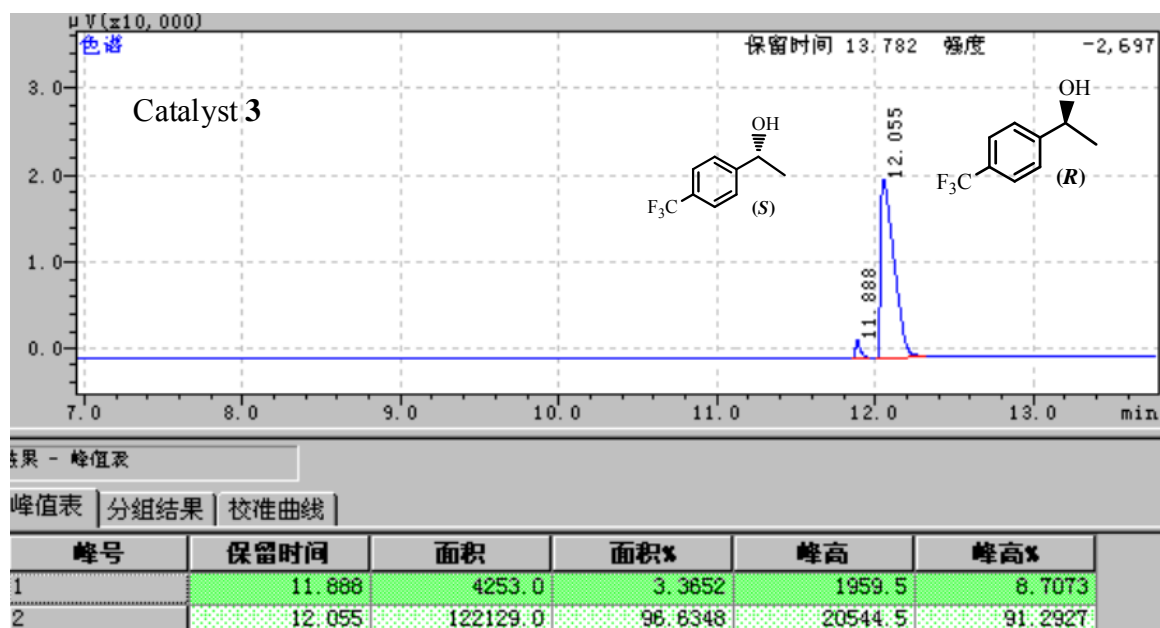
Asymmetric transfer hydrogenation of 3-methoxyacetophenone.



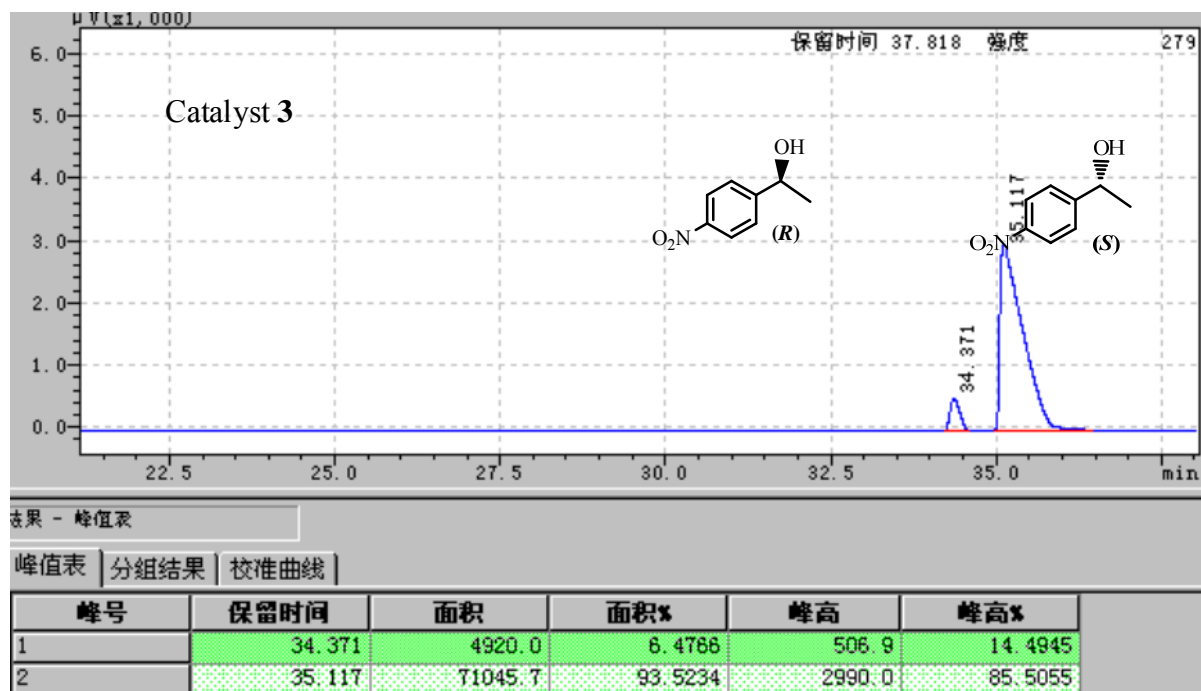
Asymmetric transfer hydrogenation of 4-cyanoacetophenone.



Asymmetric transfer hydrogenation of 4-trifluoromethylacetophenone.



Asymmetric transfer hydrogenation of 4-nitroacetophenone.



Asymmetric transfer hydrogenation of 2-acetonaphthone. (Daicel OJ-H chiralcel columns: 1.0 mL/min, 2-propanol: n-hexane=7:93, T=40 °C.) ref: [Liu, P. N.; Gu, P. M.; Wang F.; Tu, Y. Q. Org. Lett., 2004, 6, 169.].

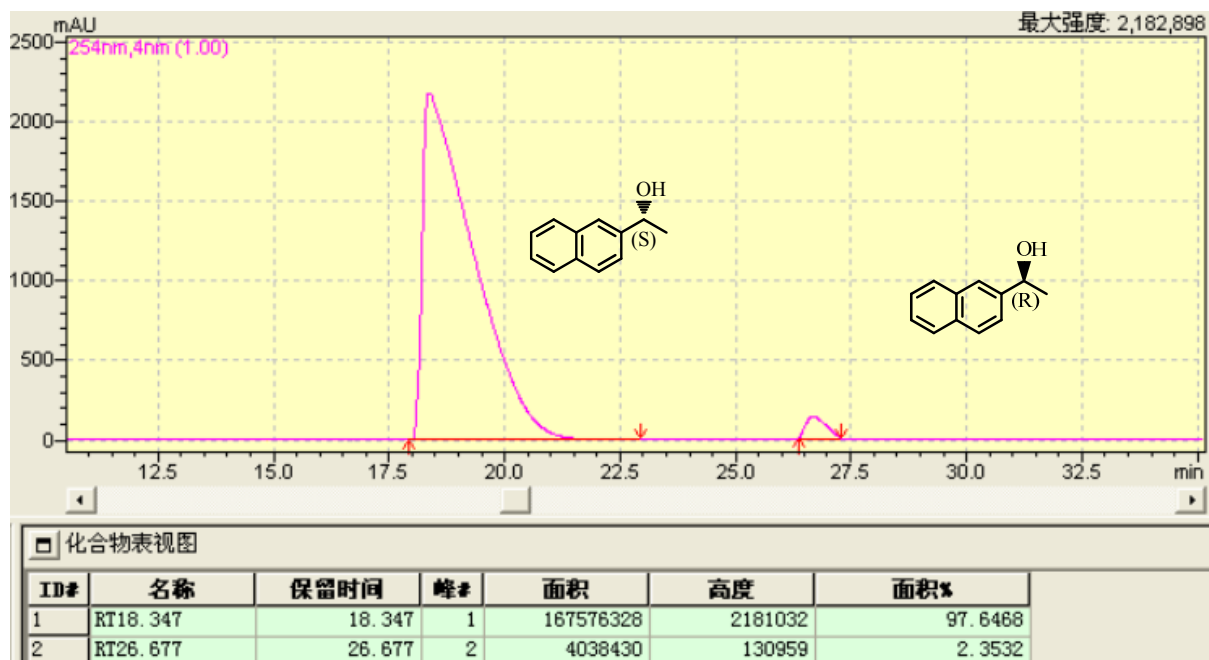
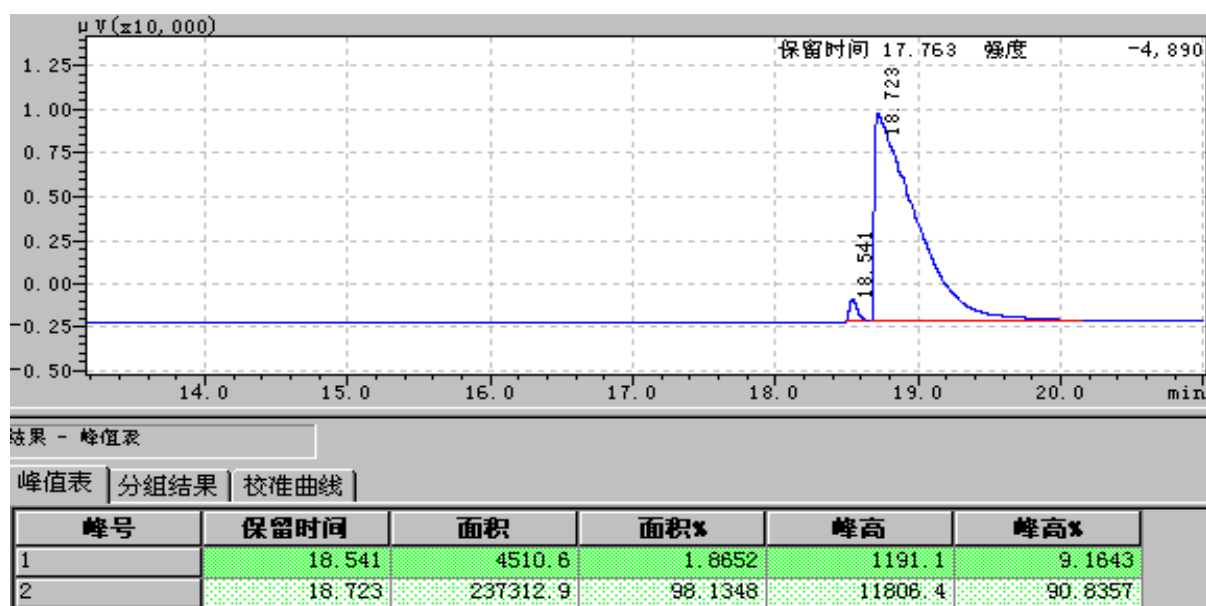


Table S1. Reusability of the catalyst **3** using acetophenone as a substrate.

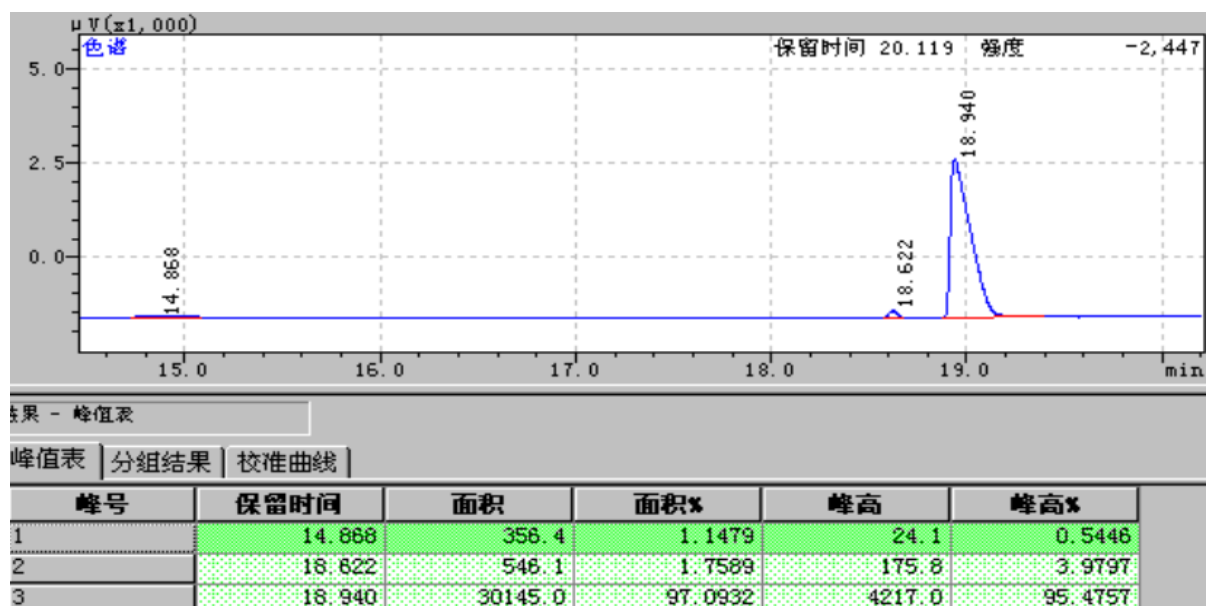
Run	1	2	3	4	5	6	7	8	9	10	11	12
Conv.	99.9	99.9	98.9	99.4	99.9	99.8	99.9	99.9	99.4	99.9	99.9	99.9
E.e	96.8	96.2	96.4	96.2	96.2	96.0	95.7	95.7	95.2	94.5	94.6	93.2

Figure S7. Reusability of the catalyst **3** using acetophenone as a substrate.

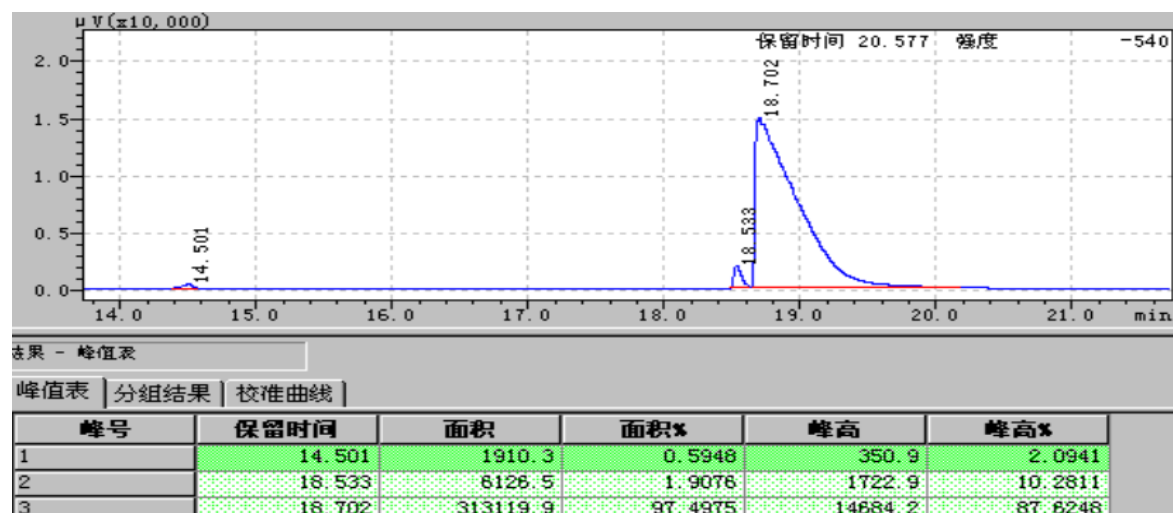
Recycle 2 of the catalyst **3** using acetophenone as a substrate.



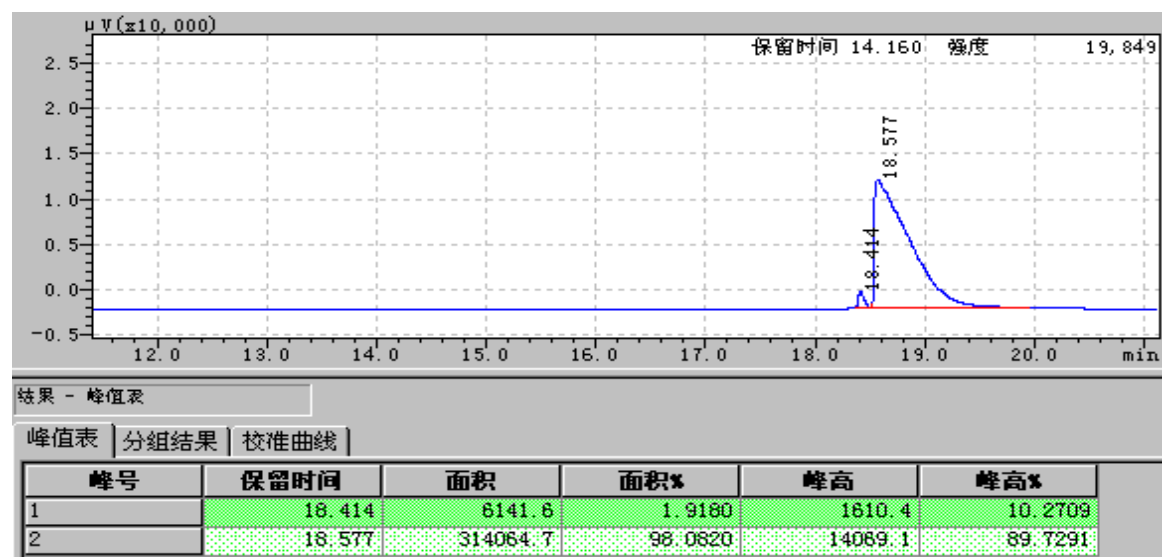
Recycle 3 of the catalyst **3** using acetophenone as a substrate.



Recycle 4 of the catalyst **3** using acetophenone as a substrate.



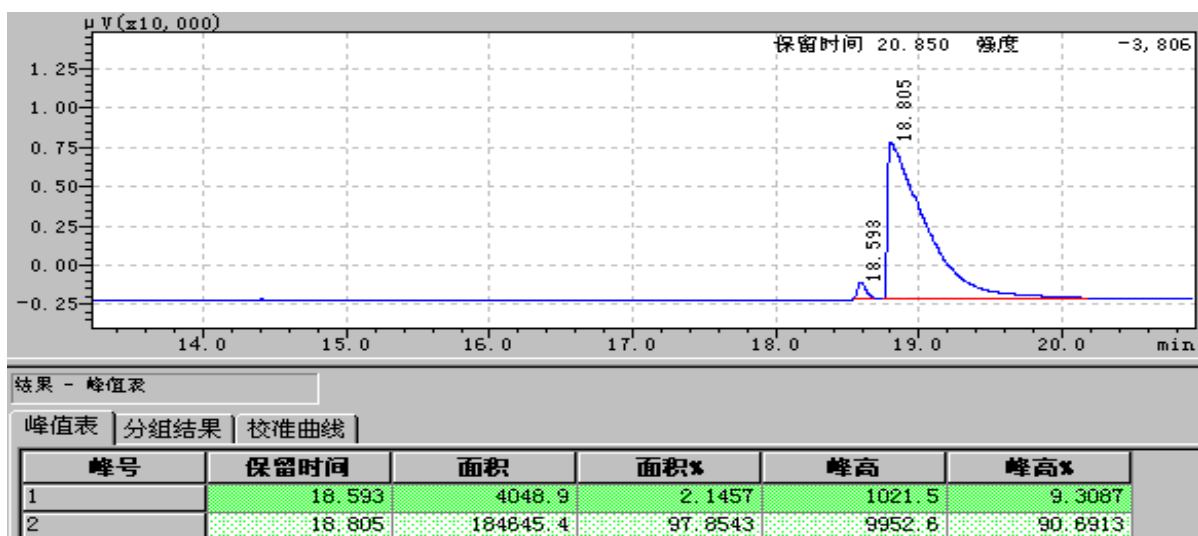
Recycle 5 of the catalyst **3** using acetophenone as a substrate.



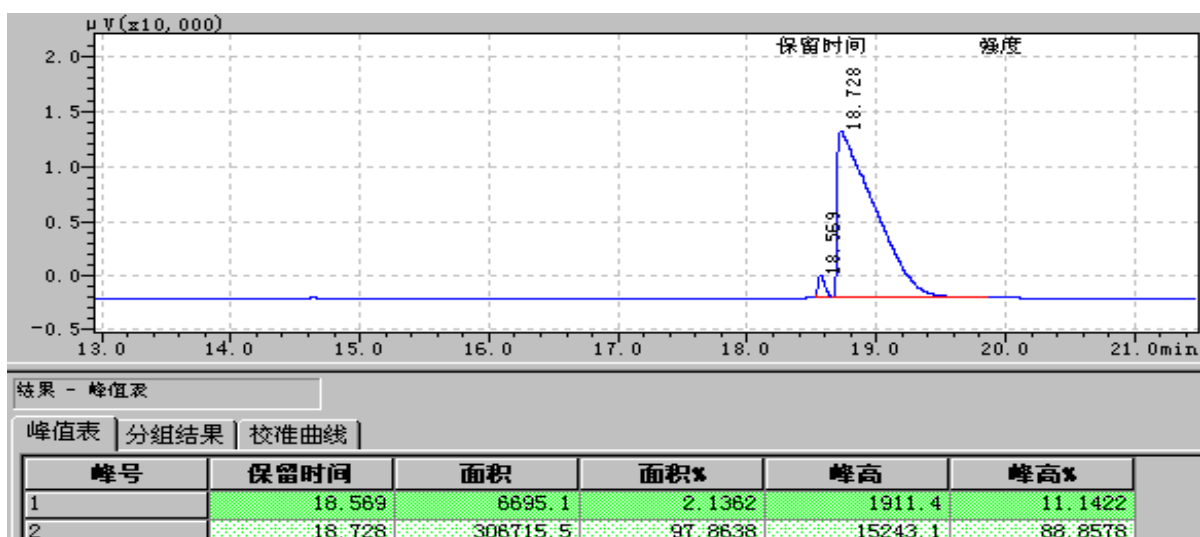
Recycle 6 of the catalyst **3** using acetophenone as a substrate.



Recycle 7 of the catalyst **3** using acetophenone as a substrate.



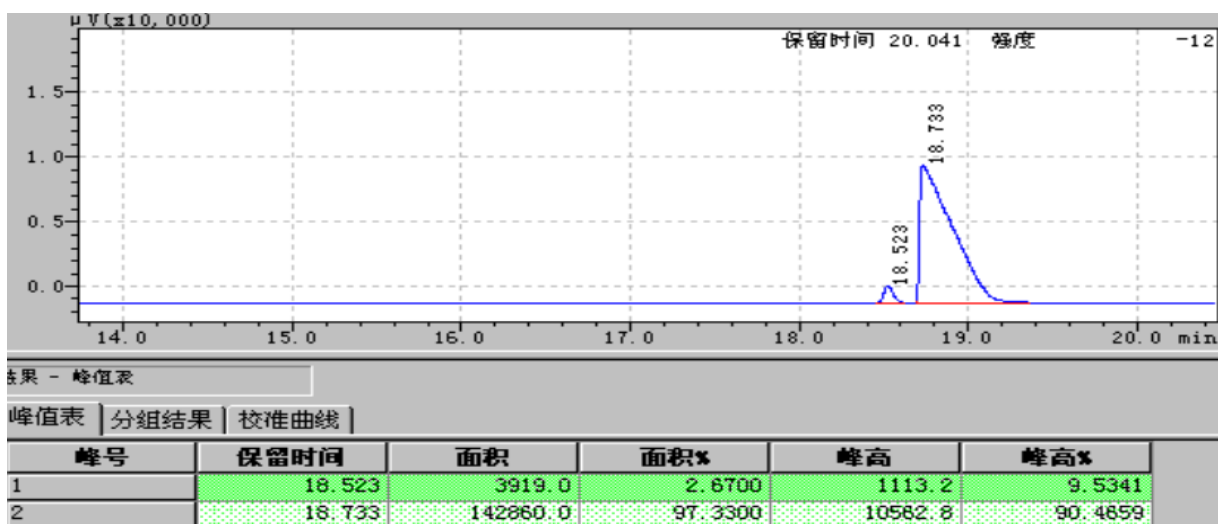
Recycle 8 of the catalyst **3** using acetophenone as a substrate.



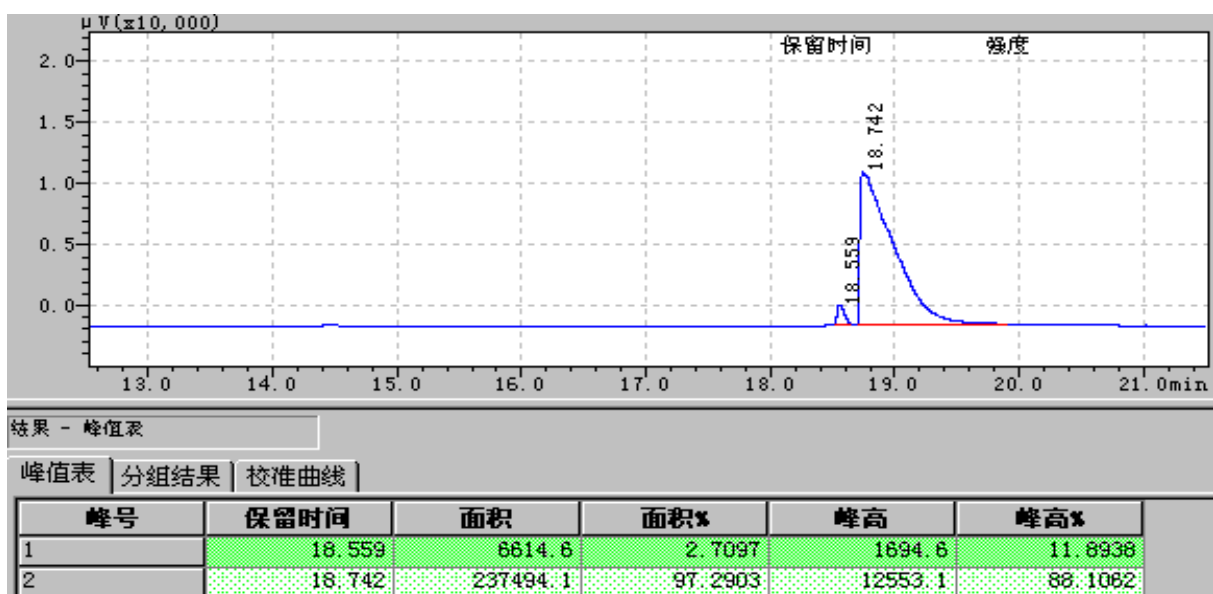
Recycle 9 of the catalyst **3** using acetophenone as a substrate.



Recycle 10 of the catalyst **3** using acetophenone as a substrate.



Recycle 11 of the catalyst **3** using acetophenone as a substrate.



Recycle 12 of the catalyst **3** using acetophenone as a substrate.

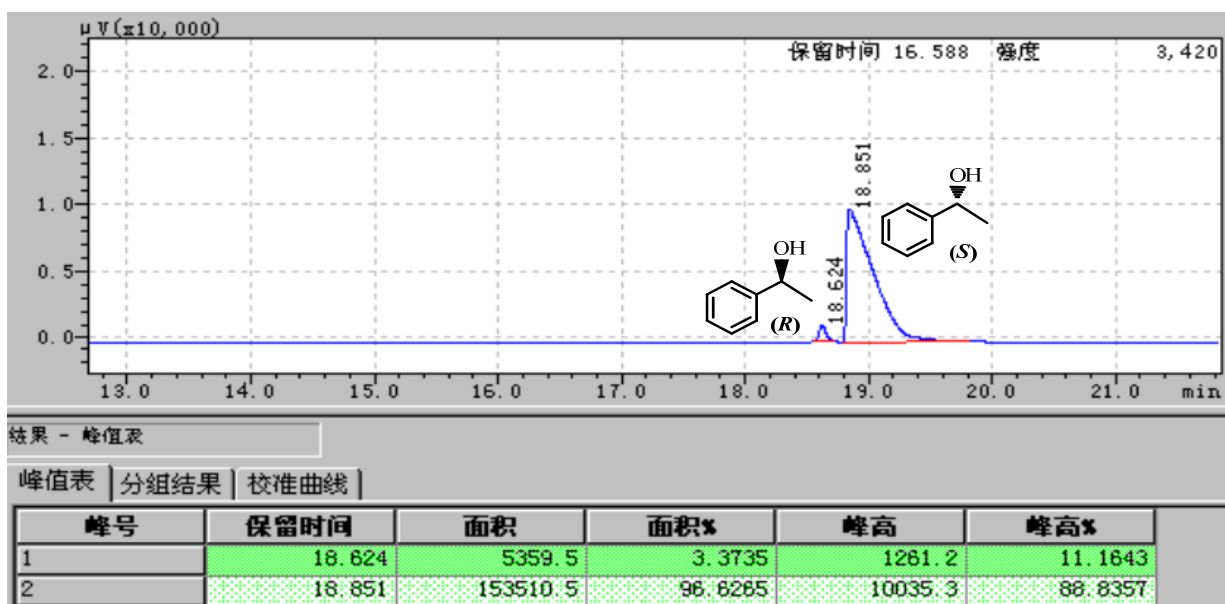
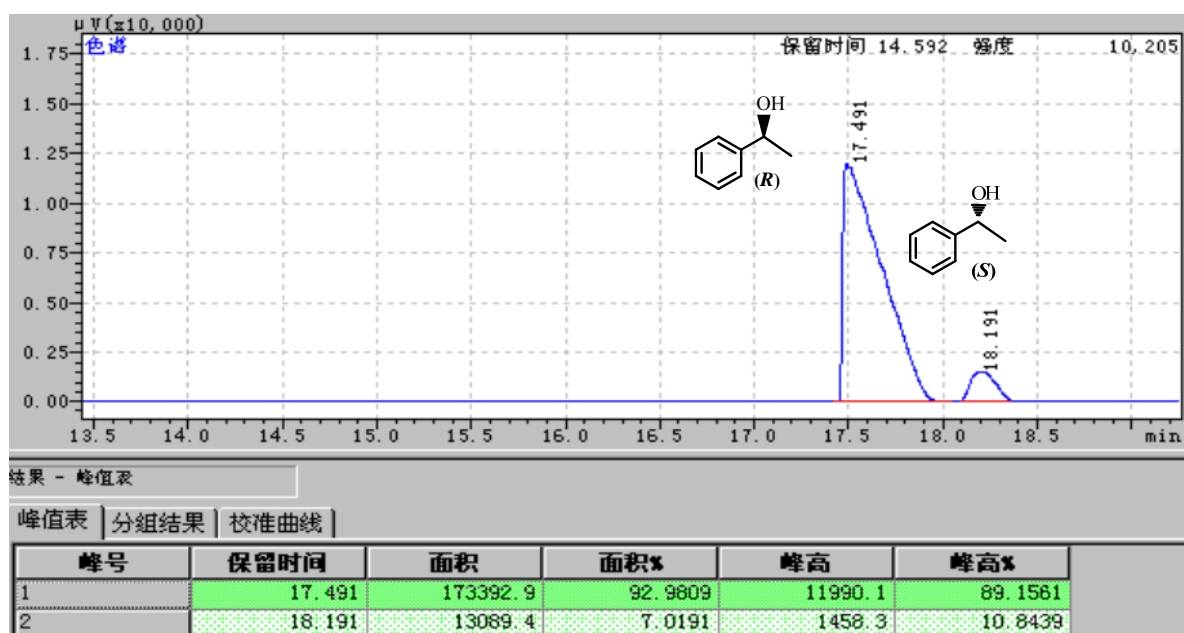


Table S2. Reusability of the catalyst **4** using acetophenone as a substrate.

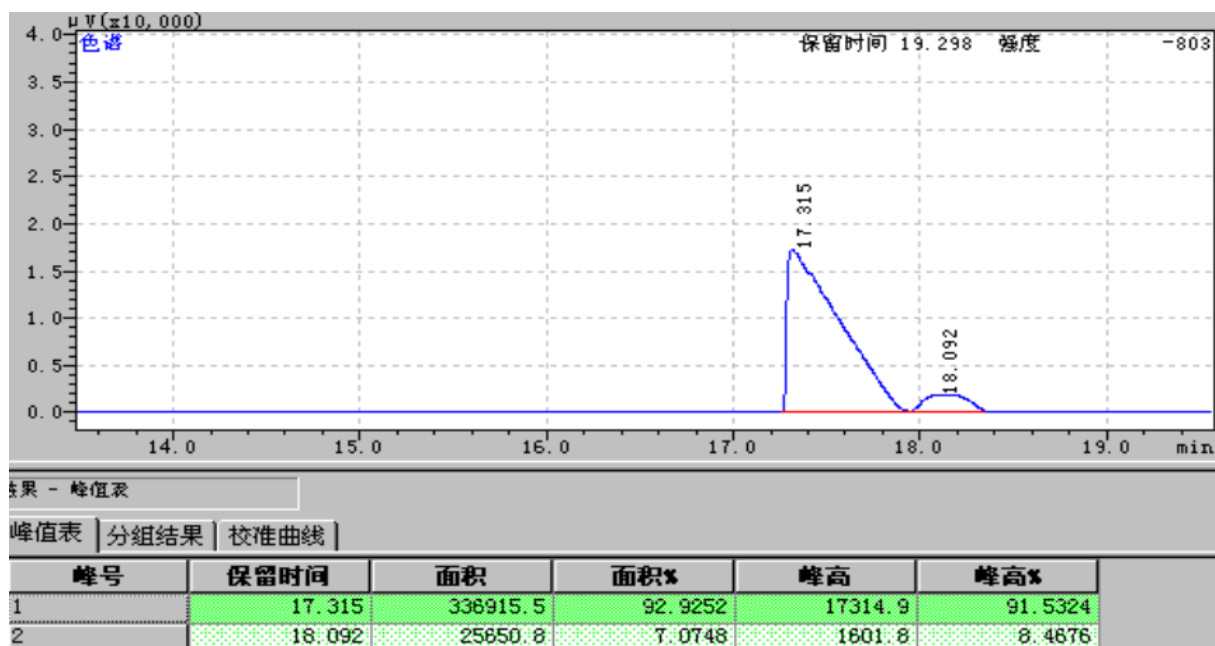
Run	1	2	3	4	5	6	7	8	9	10	11	12	13	14	15
Conv.	99.9	99.9	99.9	99.9	99.9	99.9	99.9	99.9	99.9	99.9	99.9	99.9	99.9	99.9	95.1
E.e	86.9	86.0	85.9	85.8	85.6	84.5	84.4	84.5	84.1	84.5	83.7	84.5	83.4	83.4	83.0

Figure S8. Reusability of the catalyst **4** using acetophenone as a substrate.

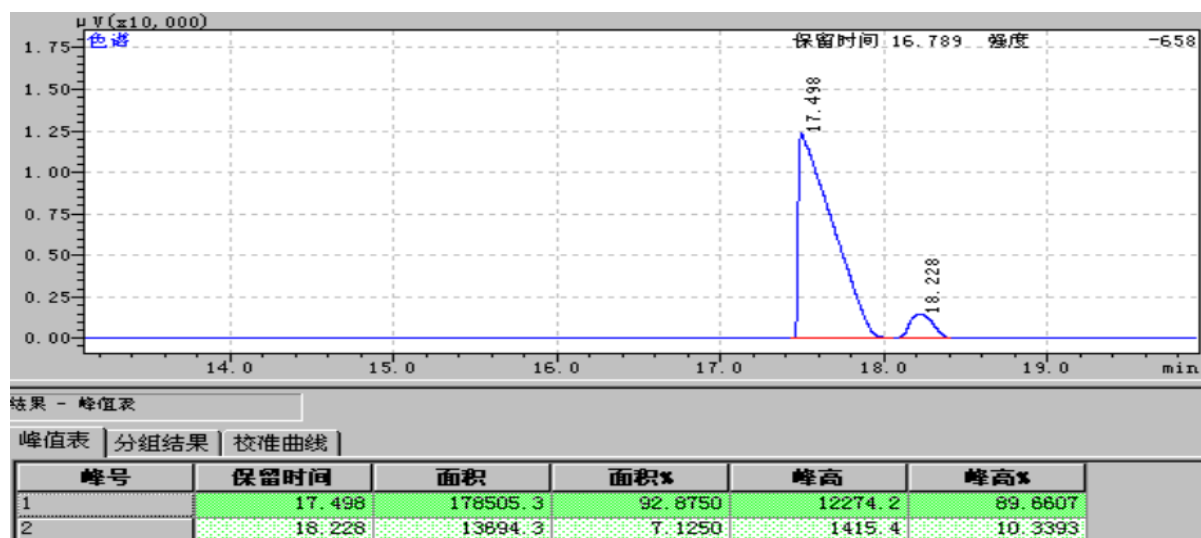
Recycle 2 of the catalyst **4** using acetophenone as a substrate.



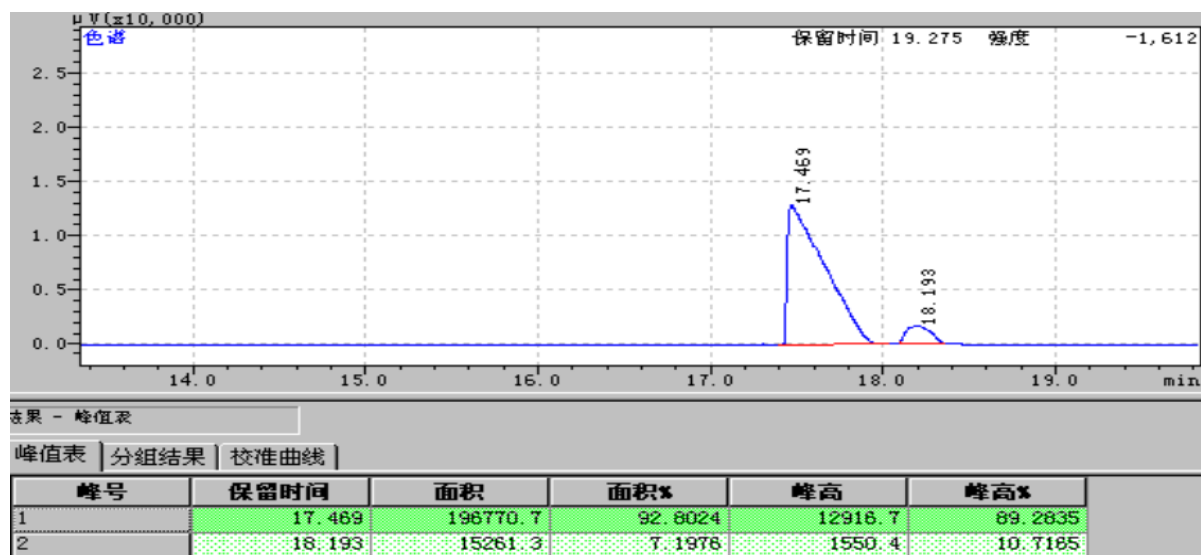
Recycle 3 of the catalyst **4** using acetophenone as a substrate.



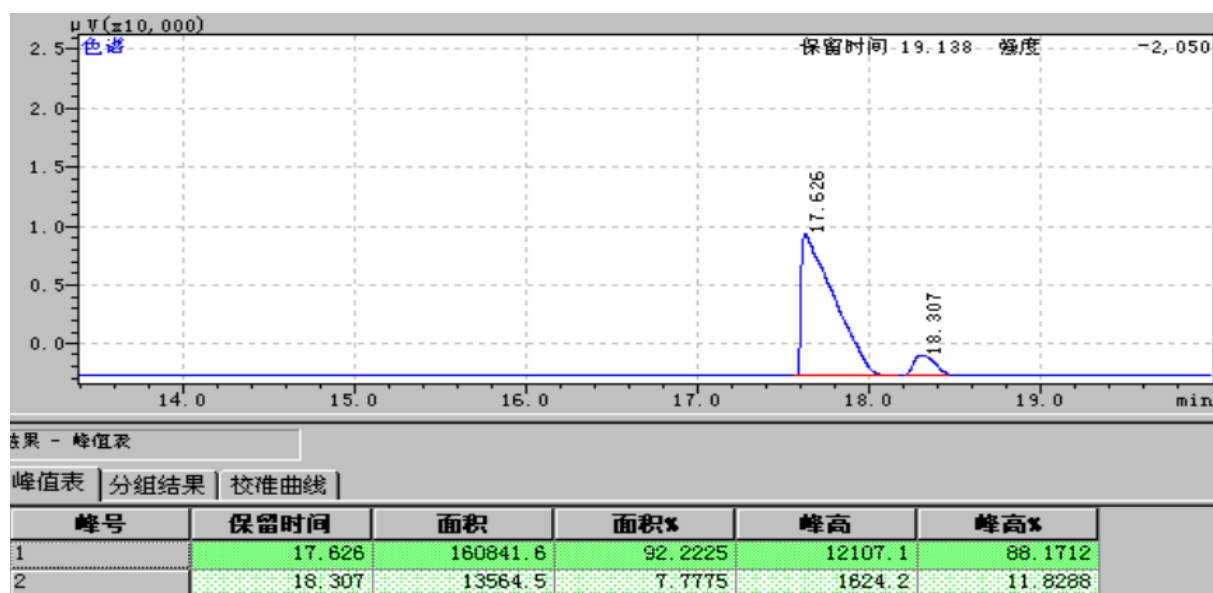
Recycle 4 of the catalyst **4** using acetophenone as a substrate.



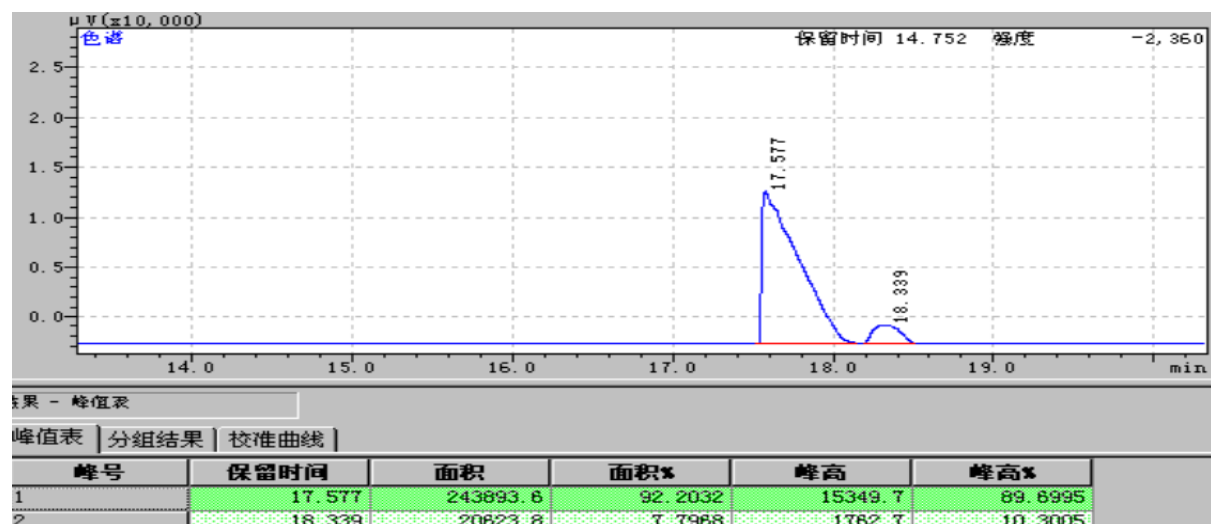
Recycle 5 of the catalyst **4** using acetophenone as a substrate.



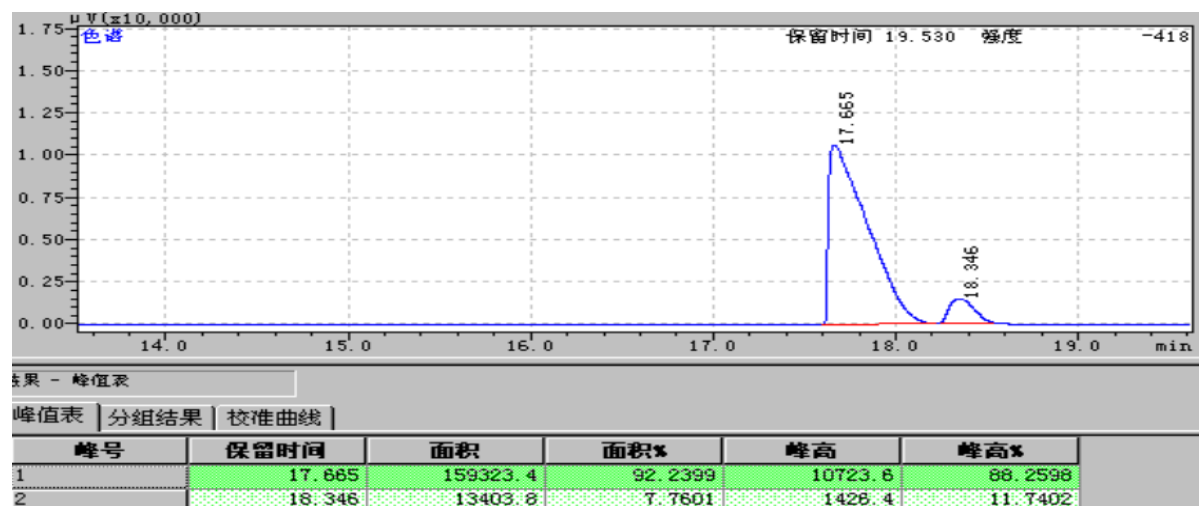
Recycle 6 of the catalyst **4** using acetophenone as a substrate.



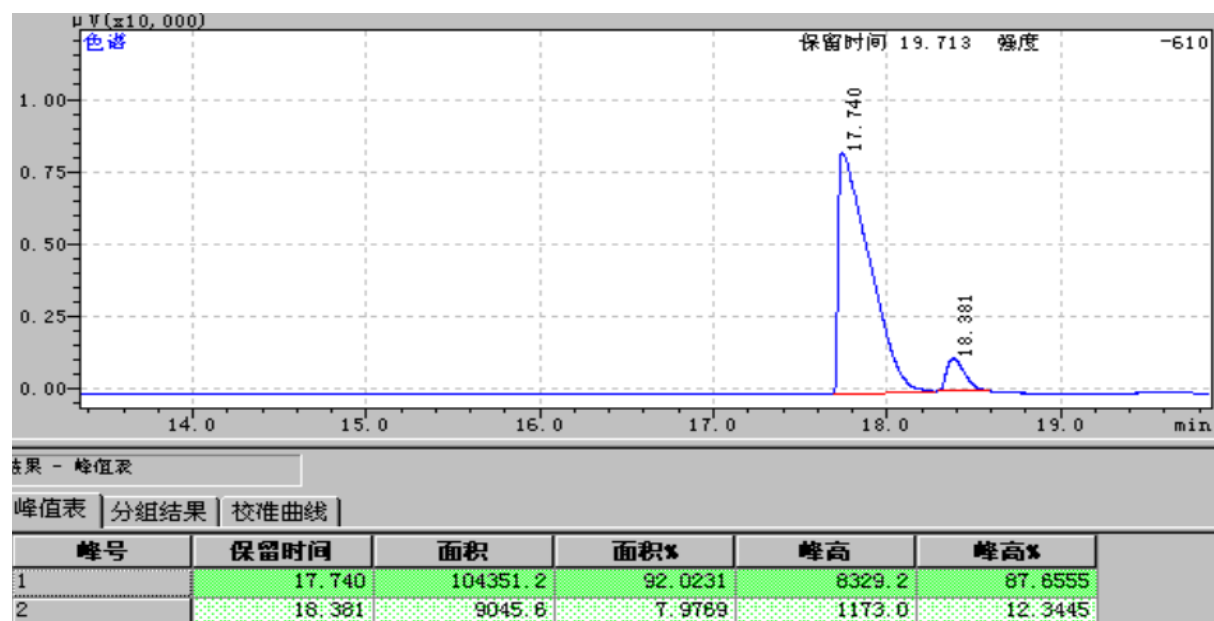
Recycle 7 of the catalyst **4** using acetophenone as a substrate.



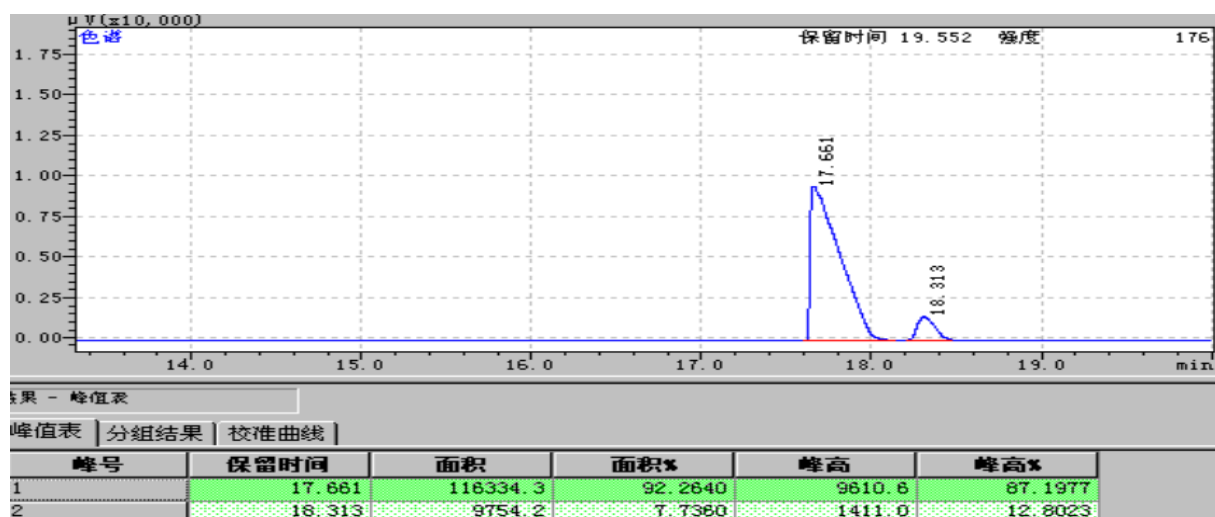
Recycle 8 of the catalyst **4** using acetophenone as a substrate.



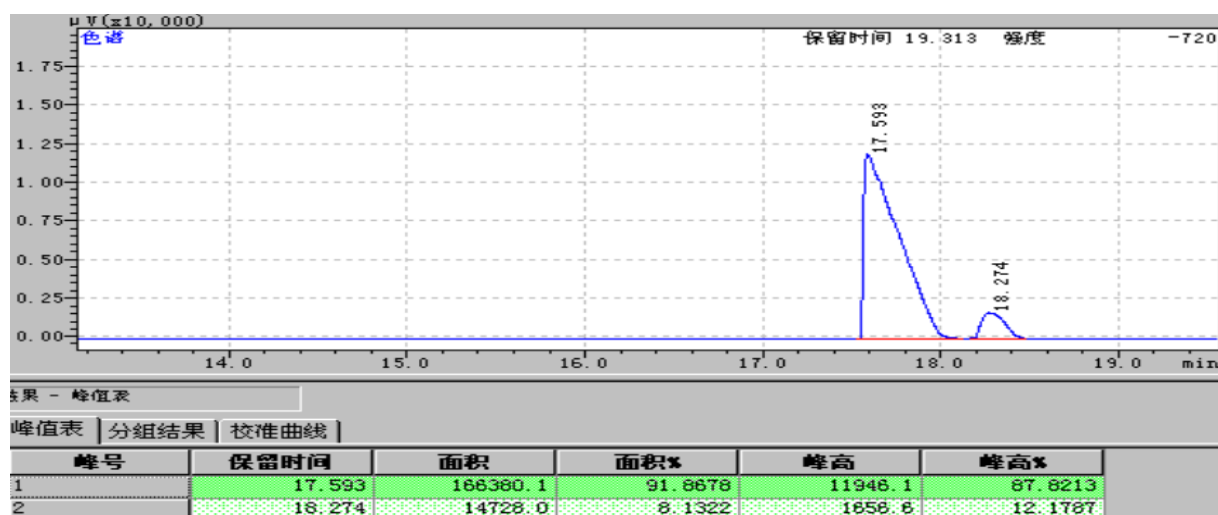
Recycle 9 of the catalyst **4** using acetophenone as a substrate.



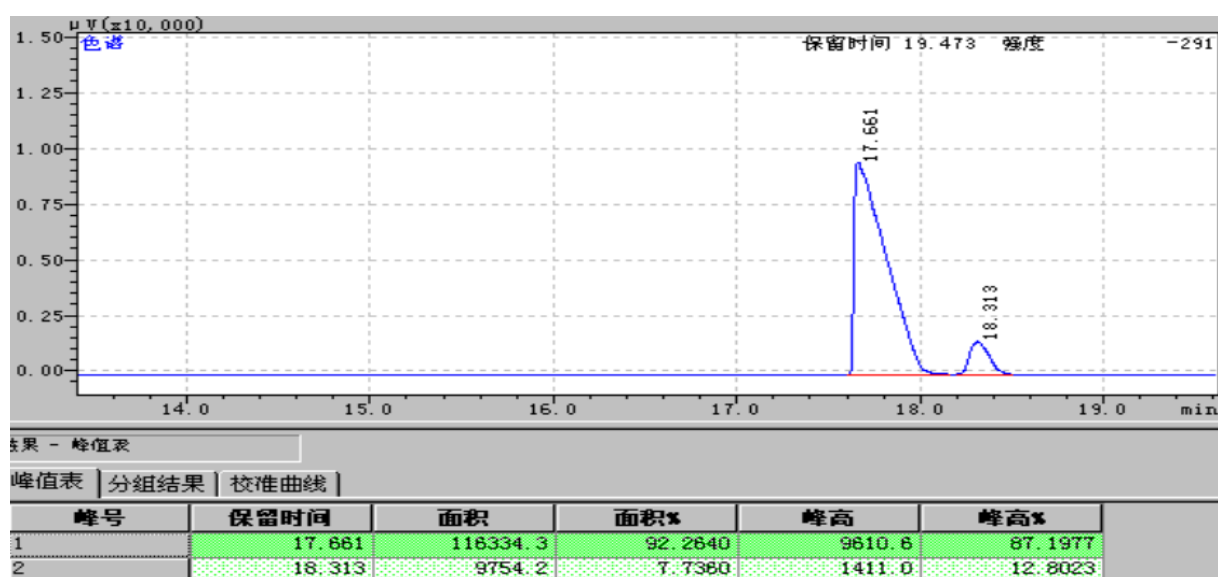
Recycle 10 of the catalyst **4** using acetophenone as a substrate.



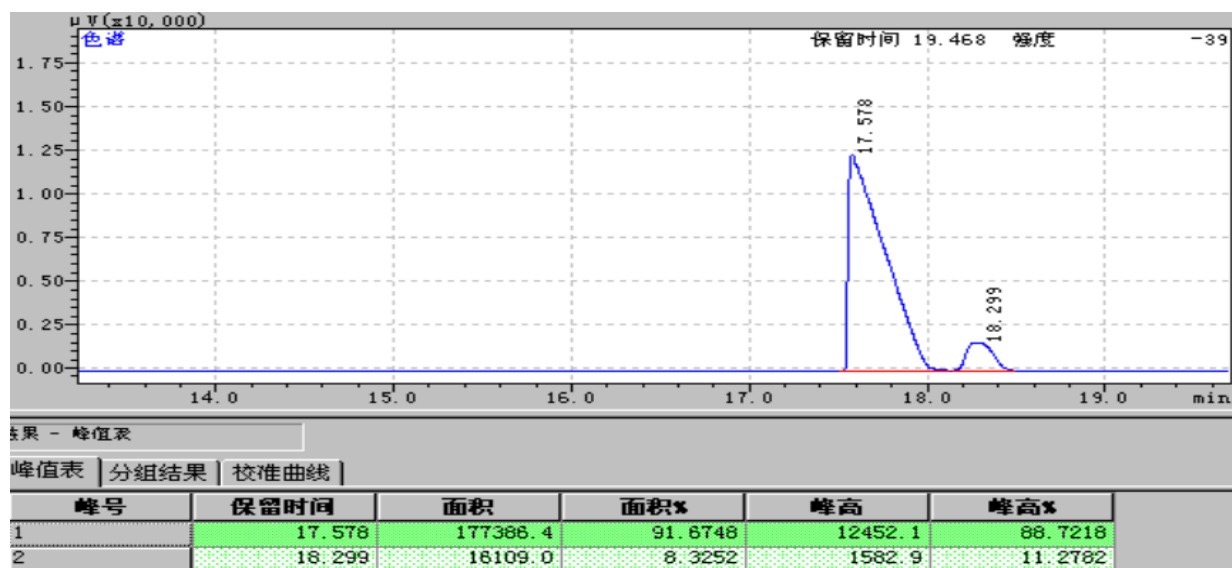
Recycle 11 of the catalyst **4** using acetophenone as a substrate.



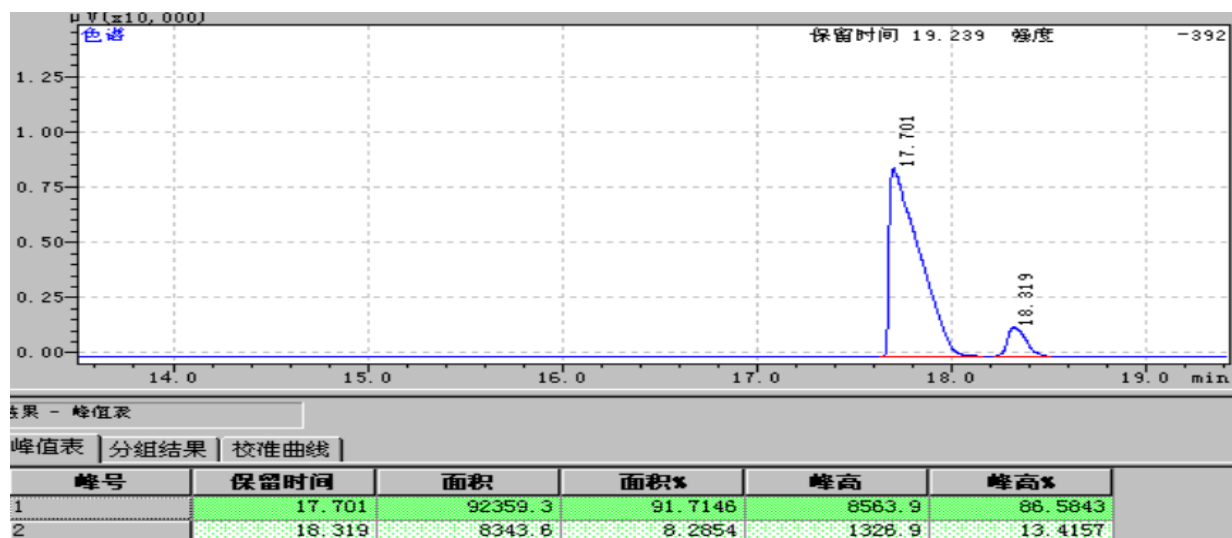
Recycle 12 of the catalyst **4** using acetophenone as a substrate.



Recycle 13 of the catalyst **4** using acetophenone as a substrate.



Recycle 14 of the catalyst **4** using acetophenone as a substrate.



Recycle 15 of the catalyst **4** using acetophenone as a substrate.

